Control Oriented Modeling for Enhanced Yaw Stability and Vehicle Steerability

Jihua Huang, Jasim Ahmed, Aleksandar Kojic, Jean-Pierre Hathout

Abstract - **Emerging drivetrains open new possibilities in vehicle stability control. In this paper, we consider a vehicle powered by four independently driven wheel motors, one for each wheel, with Steer-by-Wire. We explore the possibilities of using steering and individual wheel acceleration on top of braking to enhance stability and steerability. A 7-DOF model is developed to capture the vehicle longitudinal, lateral and yaw motion and the other four degrees of motion representing the wheel dynamics. However, this 7-DOF model is rather complicated for controller design due to the coupling of the inputs, and because the tire forces are highly nonlinear and coupled when the tires are at their limits. A control oriented model is developed that decouples the inputs and facilitates ease in control algorithm development. In addition, the longitudinal and lateral forces are also decoupled based on detailed analysis of the tire behavior at their limits. Simulation results of both the 7-DOF model and the control oriented model are compared to show that the control oriented model is capable of capturing the vehicle behavior at safety-critical cases.**

Keyword - **Vehicle Stability Control, Control oriented modelling, HSRI tire model**

I. Introduction

Vehicle Stability Control (VSC) systems have been developed since the 1980's. Their main purpose is to keep the vehicle controllable by the driver when the vehicle is at its physical limits, i.e., at the limits of adhesion between the tires and the road. In such situations, the tire behavior is extremely nonlinear and the linearized tire-wheel-brake system is even unstable. As a result, the vehicle may suddenly spin and the driver is caught by surprise. Usually the average driver tends to steer more and worsens the situation. The VSC system helps to stabilize the vehicle and maintain its steerability by creating a correcting yaw moment via controlling the slip of the individual wheels[1], [2], [3]. Commertial VSC systems are available, such as the Bosch Elctronic Stability Program (ESP) system.

However, current VSC systems are far from perfect: 1)The nonlinearities present in current mechanical brakes and combustion engines makes it difficult to achieve precise control of the tire slip; 2)Current VSC systems are not fault tolerant; if the slip control on one tire fails, the VSC has to be shut off; 3) Since braking is the primary means of control in VSC systems, the driver will experience deceleration of the vehicle even with careful braking torque distribution.

Emerging Electric Vehicles (EVs) provide new solutions to these constraints. From a controls perspective, EVs possess two advantages over traditional vehicles with internal combustion engines. Firstly, electric motors can be controlled much more precisely, over a much shorter control period than internal combustion engines. Secondly, for EVs with in-wheel motors, the individual torque of each drive wheel can be controlled independently. Therefore, in-wheel motors can directly generate a marked torque difference, making advanced dynamic yaw-moment control possible[4], [5], and [6]. However, current researches on EVs target only at normal driving conditions by assuming a small steering angle and using a linear tire model.

The challenges in VSC system design are mainly two-folded. One is that under extreme driving conditions, the tire forces are nonlinear and the longitudinal and lateral tire forces are highly coupled. The other is that the inputs, which are the steering angle and the four torques from the wheel motors, are also coupled. In [8], a heuristic based non-linear control algorithm was developed. To facilitate ease in control design we employ a different approach in this paper where instead of handling these difficulties in the controller design, a control-oriented modeling approach is proposed. In this approach, control strategies are incorporated to decouple both the tire forces and the inputs. The goal is to achieve the balance between model fidelity and model simplicity.

The paper is organized as follows: a full model is derived in Section II and then simplified into a 7-DOF model with some general assumptions in Section III. Section IV and V introduce the control-oriented modeling, with details in the decoupling of the tire longitudinal and lateral forces and the decoupling of the inputs. Simulation results are shown in Section VI to prove the effectiveness of the control-oriented modeling. Conclusions are given at the end of the paper.

Jihua Huang is with Mechanical Engineering, University of California at Berkeley, Berkeley, CA 94710, USA jihua@newton.berkeley.edu

Jasim Ahmed, Aleksandar Kojic and Jean-Pierre Hathout are with Robert Bosch Corporation, Research and Technology Center North America, 4009 Miranda Avenue, Palo Alto, CA 94304, USA Jasim.Ahmed@rtc.bosch.com

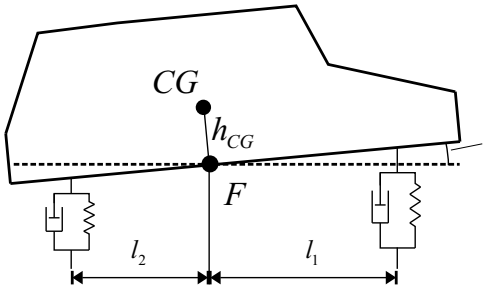

Fig. 1. Pitch and roll center

II. The Full Vehicle Model

In this section, we develop a complete model for the front-steering, 4-wheel independently driven vehicle.

The equations of motion of the vehicle are expressed in a frame fixed to the vehicle unsprung mass, E^u, which results from rotating an inertial frame E^{IN} by a yaw angle ψ. The frame E^u is fixed at the roll and pitch center of the vehicle given by F in Figure 1. A third frame E^s fixed to the vehicle sprung mass and is obtained by rotating E^u by a pitch angle θ and then a roll angle ϕ. The relationship between the various frames and the expression for the position of the center of gravity and its derivatives in the E^u frame are given by

$$E^u = \begin{bmatrix} cos\psi & sin\psi & 0 \\ -sin\psi & cos\psi & 0 \\ 0 & 0 & 1 \end{bmatrix} E^{IN}$$

$$E^s = \begin{bmatrix} 1 & 0 & 0 \\ 0 & cos\phi & sin\phi \\ 0 & -sin\phi & cos\phi \end{bmatrix} \begin{bmatrix} cos\theta & 0 & -sin\theta \\ 0 & 1 & 0 \\ sin\theta & 0 & cos\theta \end{bmatrix} E^u$$

$$r_{CG} = r_F + h_{CG} e_3^s$$

$$\dot{r}_{CG} = \dot{r}_F + h_{CG}\dot{e}_3^s = \begin{bmatrix} v_x & v_y & v_z \end{bmatrix} \begin{bmatrix} e_1^u \\ e_2^u \\ e_3^u \end{bmatrix} + h_{CG}\dot{e}_3^s$$

$$\ddot{r}_{CG} = \begin{bmatrix} \dot{v}_x - v_y\dot{\psi} & \dot{v}_y + v_x\dot{\psi} & \dot{v}_z \end{bmatrix} \begin{bmatrix} e_1^u \\ e_2^u \\ e_3^u \end{bmatrix} + h_{CG}\ddot{e}_3^s$$

$$= \begin{bmatrix} \dot{v}_x - v_y\dot{\psi} + h_{CG}(\ddot{\theta} + 2\dot{\psi}\dot{\phi}) \\ \dot{v}_y + v_x\dot{\psi} + h_{CG}(-\ddot{\phi} + 2\dot{\psi}\dot{\theta}) \\ \dot{v}_z + h_{CG}(-(\dot{\psi})^2 - (\dot{\theta})^2) \end{bmatrix}^T \begin{bmatrix} e_1^u \\ e_2^u \\ e_3^u \end{bmatrix}$$

In the above derivation, we have assumed that the pitch and roll motion is small so that $sin\theta \approx \theta$, $cos\theta \approx 1$, $sin\phi \approx \phi$, $cos\phi \approx 1$. Using these relationships, we then obtain the translational equations of motion in the E^u frame,

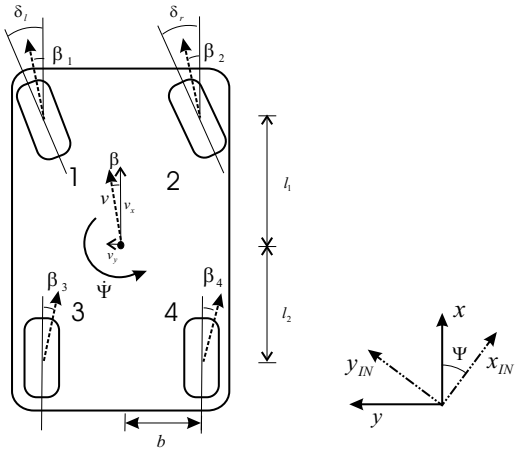

Fig. 2. Vehicle Model

$$\sum_{i=1}^{4} F_{xi} = m(\dot{v}_x - v_y\dot{\psi} + h_{CG}(\ddot{\theta} + 2\dot{\psi}\dot{\phi})) \quad (1)$$

$$\sum_{i=1}^{4} F_{yi} = m(\dot{v}_y + v_x\dot{\psi} + h_{CG}(-\ddot{\phi} + 2\dot{\psi}\dot{\theta})) \quad (2)$$

$$\sum_{i=1}^{4} F_{zi} - mg = m(\dot{v}_z + h_{CG}(-(\dot{\psi})^2 - (\dot{\theta})^2)) \quad (3)$$

where m is the mass of the vehicle and the wheels, v_x, v_y, v_z are the components of the vehicle velocity at F expressed in E^u and h_{CG} is the distance between F and CG, the center of gravity of the vehicle. The forces F_{xi} and F_{yi}, $i = 1, \ldots, 4$, are the tire forces in the vehicle longitudinal and lateral directions (in E^u).

Similarly, the rotational equations of motion (in E^s) are given by,

$$M_1 = b(F_{z1} + F_{z3} - F_{z2} - F_{z4}) = I_x\ddot{\phi} + (I_z - I_x - I_y)\dot{\theta}\dot{\psi} \quad (4)$$

$$M_2 = -l_1(F_{z1} + F_{z2}) + l_2(F_{z3} + F_{z4}) = I_y\ddot{\theta} + (I_x + I_y - I_z)\dot{\phi}\dot{\psi} \quad (5)$$

$$M_3 = l_1(F_{y1} + F_{y2}) - l_2(F_{y3} + F_{y4}) + b(F_{x2} + F_{x4} - F_{x1} - F_{x3}) = I_z\ddot{\psi} + (I_y - I_x - I_z)\dot{\phi}\dot{\theta} \quad (6)$$

where I_x, I_y, and I_z are the moments of inertia about e_1^s, e_2^s, and e_3^s, respectively, and M_i is the moment about e_i^s, $i = 1, \ldots, 3$.

The wheel dynamics are given by

$$J_{wi}\dot{\omega}_i = T_i - F_{ai}r \ , \ i = 1, \ldots, 4, \quad (7)$$

where ω_i is the wheel rotational speed for the ith wheel; J_{wi} is the moment of inertia of the ith wheel and its

corresponding drivetrain and motor; T_i is the motor torque, and F_{ai} is the tire longitudinal force, i.e., the tire force in the tire plane along the longitudinal direction.

III. The 7DOF Vehicle Model

Our primary interest in VSC is to control the vehicle's lateral and yaw motion. In this section, we will make the following general assumptions to simplify the full model:

- We ignore roll, pitch and bounce motion to obtain

$$\sum_{i=1}^{4} F_{xi} = m(\dot{v}_x - v_y\dot{\psi} + h_{CG}(\ddot{\theta} + 2\dot{\psi}\dot{\phi}))$$
$$\sum_{i=1}^{4} F_{yi} = m(\dot{v}_y + v_x\dot{\psi} + h_{CG}(-\ddot{\phi} + 2\dot{\psi}\dot{\theta}))$$
$$M_3 = I_z\ddot{\phi} = l_1(F_{y1} + F_{y2}) - l_2(F_{y3} + F_{y4}) + b(F_{x2} + F_{x4} - F_{x1} - F_{x3})$$

  With this assumption, v_x and v_y are also the longitudinal and lateral velocities at vehicle CG.

- Next, we ignore aerodynamic forces and the rolling resistance of the tires to obtain,

$$F_{xi} = F_{ai}\cos(\delta) - F_{si}\sin(\delta)\ ,\ i = 1,2$$
$$F_{yi} = F_{ai}\sin(\delta) + F_{si}\cos(\delta)\ ,\ i = 1,2$$
$$F_{xi} = F_{ai}\ ,\ i = 3,4$$
$$F_{y1} = F_{si}\ ,\ i = 3,4$$

  where F_{ai} and F_{si} are the tire longitudinal force and tire lateral force for the ith wheel ($i = 1,\ldots,4$), respectively.

- Finally, we assume that the steering angle is small, i.e., $sin\delta \approx \delta$ and $cos\delta \approx 1$, so that,

$$F_{xi} = F_{ai} - F_{si}\delta\ ,\ i = 1,2$$
$$F_{yi} = F_{ai}\delta + F_{si}\ ,\ i = 1,2$$
$$F_{xi} = F_{ai}\ ,\ i = 3,4$$
$$F_{y1} = F_{si}\ ,\ i = 3,4$$

With these assumptions, we derive a 7DOF model:

$$\dot{v}_x = v_y\omega_z + \frac{1}{m}(\sum_{i=1}^{4} F_{ai} - \delta(F_{s1} + F_{s2})) \quad (8)$$

$$\dot{v}_y = -v_x\omega_z + \frac{1}{m}(\sum_{i=1}^{4} F_{si} + \delta(F_{a1} + F_{a2})) \quad (9)$$

$$\dot{\omega}_z = \frac{1}{I_z}(l_1(F_{s1} + F_{s2}) - l_2(F_{s3} + F_{s4}) + b\delta(F_{s1} - F_{s2}) + l_1\delta(F_{a1} + F_{a2}) + b(F_{a2} + F_{a4} - F_{a1} - F_{a3})) \quad (10)$$

$$\dot{\omega}_i = \frac{1}{J_{wi}}(T_i - F_{ai}r)\ ,\ i = 1,\ldots,4 \quad (11)$$

where $\omega_z = \dot{\psi}$ is the yaw velocity, δ and T_i represent the control inputs. δ is the front steering angle and T_i the torques of the four independently driven in-wheel motors $i = 1,\ldots,4$.

The 7-DOF model is rather complicated for controller design because the tire forces F_{ai} and F_{si} are highly nonlinear functions of the vehicle states and control inputs, and are coupled to each other. To facilitate controller design, a simpler model is preferred. In this paper, the model is further simplified by carefully examining the nonlinear function of the tire forces and incorporating certain control strategies. The next two section describe these in detail.

IV. Decoupling of the Tire Forces

Though there are various tire models to describe tire behavior, these models generally treat tire forces as functions of tire longitudinal slip ratio λ and tire slip angle α which is the angle between the wheel plane and the velocity at the wheel center. Other factors that affect the tire forces, such as the normal force and the tire/road friction coefficient, are incorporated in the tire model as parameters. Hence, we write the tire longitudinal and lateral force as follows (for front steering vehicles only),

$$F_{ai} = F_{ai}(\lambda_i, \alpha_i)\ ,\ i = 1,2,3,4$$
$$F_{si} = F_{si}(\lambda_i, \alpha_i)\ ,\ i = 1,2,3,4$$
$$\alpha_i = \begin{cases} \delta - \beta_i & i = 1,2 \\ -\beta_i & i = 3,4 \end{cases}$$

where δ is the front steering angle and β_i is the vehicle side slip angle of the ith wheel as shown in Figure 2. The side slip angle is the angle between the velocity at the wheel center and the vehicle's longitudinal axis.

Both λ_i and β_i can be calculated from vehicle states or their estimates [9]. We assume that the velocity of each wheel is the vehicle's longitudinal velocity v_x, so that,

$$\lambda_i = \frac{\omega_i r - v_x}{v_x}\ ,\quad i = 1,\ldots,4$$

where r is the wheel effective radius. Further, assume that β_i is small, i.e. $\beta_i \approx tan\beta_i$, and $v_x >> b\omega_z$, so that

$$\beta_1 = \beta_2 = \frac{v_y + l_1\omega_z}{v_x}$$
$$\beta_3 = \beta_4 = \frac{v_y - l_2\omega_z}{v_x}$$

However, this simplification does not help with the fact that the tire forces are nonlinear, and that the lateral and longitudinal forces are highly coupled when the tires approach their physical limits. A good tire model that captures the coupling of the tire longitudinal and lateral forces is the

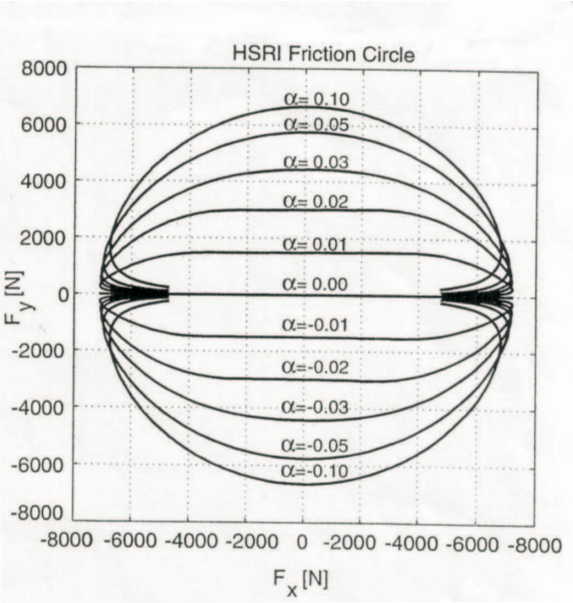

Fig. 3. HSRI tire model friction circle

HSRI tire model [7],

$$\mu = \mu_{peak}(1 - A_s R\omega\sqrt{\lambda^2 + tan^2\alpha}) \quad (12)$$

$$H = \sqrt{\left(\frac{C_\lambda \lambda}{\mu F_z(1-\lambda)}\right)^2 + \left(\frac{C_\alpha tan\alpha}{\mu F_z(1-\lambda)}\right)^2} \quad (13)$$

$$F_a = \begin{cases} C_\lambda \frac{\lambda}{1-\lambda} & H < \frac{1}{2} \\ C_\lambda \frac{\lambda}{1-\lambda}\left(\frac{1}{H} - \frac{1}{4H^2}\right) & H \geq \frac{1}{2} \end{cases} \quad (14)$$

$$F_s = \begin{cases} C_\alpha \frac{1}{1-\lambda} tan(\alpha) & H < \frac{1}{2} \\ C_\alpha \frac{1}{1-\lambda} tan(\alpha)\left(\frac{1}{H} - \frac{1}{4H^2}\right) & H \geq \frac{1}{2} \end{cases} \quad (15)$$

where C_λ and C_α are the longitudinal and cornering stiffnessses, repectively, λ is the tire slip ratio, α the tire slip angle, μ_{peak} is the peak road friction, A_s is a friction discount factor due to sliding in the patch, r is the tire effective radius, and ω is the tire angular velocity. The expressions for F_a and F_s are calculated for each tire. Figure 3 shows representative tire curves from this model for a single axle.

When the slip ratio λ and the slip angle α are small, the coupling between F_a and F_s is weak, and can be ignored. However, when either λ or α is relatively large, the coupling can not be ignored. In this case, the HSRI tire model can be written as:

$$F_a = \frac{C_\lambda \lambda}{\sqrt{(C_\lambda\lambda)^2 + (C_\alpha\alpha)^2}} F_R$$

$$F_s = \frac{C_\alpha \alpha}{\sqrt{(C_\lambda\lambda)^2 + (C_\alpha\alpha)^2}} F_R$$

with F_R the resultant tire force: $F_R = \sqrt{F_a^2 + F_s^2}$.

The main task of VSC as an active safety system is to limit the vehicle side slip angle β in order to prevent the vehicle from spinning. One of the strategies VSC systems employ is to adjust the yaw moment on the car by controlling the value of the slip ratio at each wheel [1], [2]. Consider the case a free rolling tire, i.e $\lambda = 0$, reaching its limit in the lateral direction at some $\alpha = \alpha_0$ so that $F_s(\lambda = 0, \alpha_0) = F_{smax}$. If a braking torque is forced upon the wheel, a brake slip λ_0 is generated and the lateral force is reduced to $F_s(\lambda_0, \alpha_0)$ while the longitudinal force rises from 0 to $F_a(\lambda_0, \alpha_0)$ (assuming that neither the normal force F_N nor the tire slip angle α_0 changes). Note that since the lateral force reaches its limit, the addition of a small longitudinal slip does not appreciably affect the magnitude of the lateral force so that the magnitude of the resultant force does not appreciably change. However, the magnitude of the longitudinal force changes signficantly, which causes a change in the direction of the resultant force. Figure 3 shows this phenomenon. When the tire slip angle is relatively large and the slip ratio is small, the curve can be approximated by a segment of a circle with the fast changing direction parallel to the F_x(longitudinal force) axis.

The influence of applying a small slip ratio λ is now obvious: it induces the rotation of the resultant force on the tire, thus changing the yaw moment on the car. The controller needs to resolve by what amount the slip at each tire needs to be changed by to generate the required change in the yaw moment, and to mitigate the effects of this change on the longitudinal and lateral motions. Thus, a more straightforward relation between the tire forces and the slip ratio would benefit the control design.

Note that at the tire friction limits, there are no significant change in the magnitudes of $F_R(0, \alpha_0)$ and $F_R(\lambda, \alpha_0)$ so that we assume that $F_R(\lambda, \alpha_0) = constant = F_{Rmax}$ is the maximum lateral force for the rolling tires, to obtain

$$F_a = \frac{C_\lambda \lambda}{\sqrt{(C_\lambda\lambda)^2 + (C_\alpha\alpha)^2}} F_{Rmax} \quad (16)$$

Further, we assume that $C_\lambda\lambda << C_\alpha\alpha$, so that

$$F_a \approx \left(\frac{C_\lambda}{C_\alpha\alpha} F_{Rmax}\right)\lambda = K(\alpha)\lambda. \quad (17)$$

To verify that $C_\lambda\lambda << C_\alpha\alpha$ is in general true, lets consider some typical data for tires: $C_\lambda = 14,000N$ and $C_\alpha = 40,000N/rad$; the lateral force approach its limits generally at $\alpha \geq 6^o \approx 0.1rad$. With full braking, an average car experiences a deceleration of around $0.8 - 0.9g$, which is close to the tire longitudinal limits with $\lambda \approx 20\%$. With full throttle, a low-class car experiences acceleration of $0.3 - 0.4g$, and a high-class car $0.1 - 0.2g$. Hence, it is reasonable to assume that $\lambda \leq 5\%$ for yaw moment control

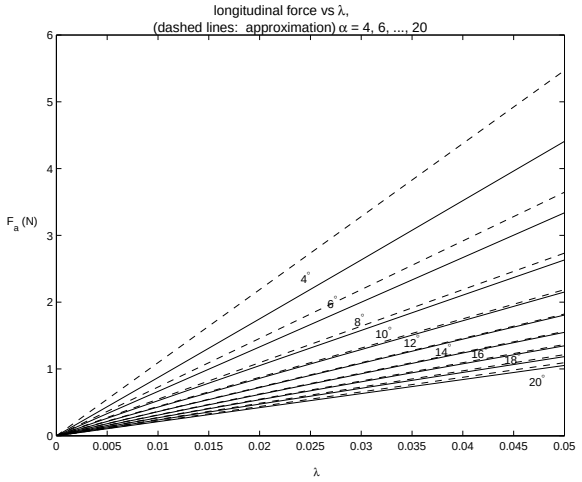

Fig. 4. Comparison of tire longitudinal force based on HSRI model and the approximation

so that

$$C_\lambda \lambda = 14000 \times 0.05 = 700N$$
$$C_\alpha \alpha = 40000 \times 0.1 = 4000N,$$
$$\Longrightarrow C_\lambda \lambda < \frac{1}{5} C_\alpha \alpha$$

Figure 4 shows both the tire longitudinal force based on the HSRI model and the longitudinal tire force based on (17). We observe that when $\lambda \leq 5\%$, the longitudinal force is approximately a linear function of λ, with the linear gain dependent on the slip angle. Note that when the tire slip angle is greater than 6^o, the approximation is very close to the HSRI result.

As the approximation (17) only occurs to the longitudinal force, the lateral force can still be caculated based on the HSRI model or other tire models. In safety-critical situations, since the longitudinal slip does not have significant effect on the lateral force, the lateral force can also be approximately as a function of the lateral slip angle only and further simplify the calculation of tire forces.

V. Control-oriented Modeling

In Section IV, the tire longitudinal force is linearized and decoupled from the tire lateral force by reasonably limiting the controlled longitudinal slip ratio λ to be smaller than 5%. However, note that in the 7-DOF complex model, the steering angle δ is coupled with the longitudinal forces, which is affected by the torque input T_i. In other words, the inputs are coupled. To make control system design easier, it is desirable to decouple the inputs. We can achieve this by incorporating some control strategies in the modeling.

The two most common conditions where the tire approaches its limit are oversteering and understeering. In the case of oversteering, the rear tires of the vehicle reach their lateral force limit while the front tires are close to but do not reach their limit. Hence, we add front tire braking/traction to affect the yaw moment, i.e. brake the outer front tire while employing traction control on the inner front tire. It is reasonable to constrain the braking and traction force to be the same, i.e., $F_{a1} = -F_{a2}$, in order to maintain the speed so that

$$F_{a1} + F_{a2} = 0 \Longrightarrow \delta(F_{a1} + F_{a2}) = 0$$

Similarly, in the case of understeering, the front tires reach the lateral force limit first. Hence braking and traction control are applied on the rear tires only so that

$$F_{a1} = F_{a2} = 0 \Longrightarrow \delta((F_{a1} + F_{a2}) = 0$$

Under both general and extreme driving conditions, the bicycle model can still be used by employing equivalent lateral forces for the front and rear lateral forces: $2F_f = (F_{s1} + F_{s2})$, and $2F_r = (F_{s3} + F_{s4})$. Assume the longitudinal velocity is a known parameter, which can be either measured or estimated, and apply $\delta(F_{a1} + F_{a2}) = 0$, so that vehicle model can be reduced to

$$\dot{v}_y = -v_x \omega_z + \frac{2}{m}(F_f + F_r) \quad (18)$$

$$\dot{\omega}_z = \frac{1}{J_z}(2l_1 F_f - 2l_2 F_r + b(F_{a2} + F_{a4} - F_{a1} - F_{a3})) \quad (19)$$

Together with the wheel dynamics (7), and the linearized tire longitudinal force function (17), these equations provide a simpler model for the control design. Furthermore, since the wheel dynamics are much faster than the vehicle dynamics, we ignore the wheel dynamics and simply determine the control input T_i based on $T_i = F_{ai} r = (K(\alpha) r)\lambda_i$.

VI. Simulation Results

We compare using numerical simulations the 7DOF model with the HSRI tire model and the control-oriented model. The simulations are conducted for our 1/5 scaled vehicle developed at Bosch [8]. In the future, we plan to compare the numerical results with experimental results of our prototype vehicle. Fig. 5 and 6 compare the simulation results of the 7-DOF model and the control oriented model. The vehicle is undergoing an extreme maneuver with a large steering angle, $\delta = 10^o$ (positive indicates a left turn), and a speed of $5m/s$ which when scaled for a regular vehicle corresponds to $25m/s$. During the time when the vehicle is oversteering i.e when the magnitude of the steering angle is 10^o, as per our control oriented modeling strategy discussed in Section V, a braking torque of -0.2Nm is applied at the outer front wheel, and a traction torque of 0.2Nm at the inner front wheel. These torque values are chosen to ensure yaw rate stability as seen in Fig. 5. Fig. 6 shows the lateral forces and side slip angles of both models (two solid lines in each subfigure correspond to the outer and inner front/rear tire forces based on the 7DOF model, one dashed line corresponds to the front/rear tire force based on the control-oriented model). We can observe from the figures that the two models match excellently.

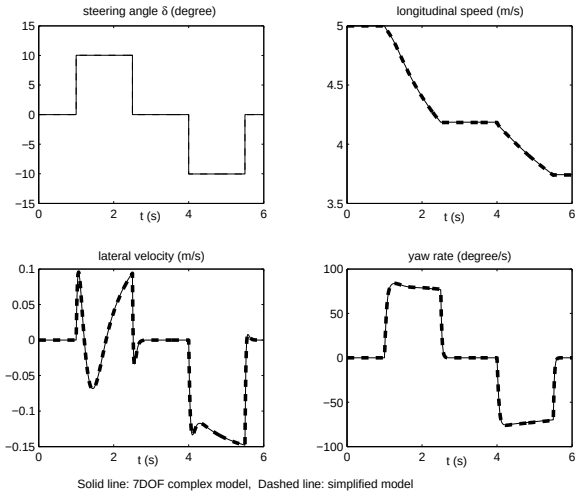

Fig. 5. Simulation results of the 7DOF model and the simplified model (a)

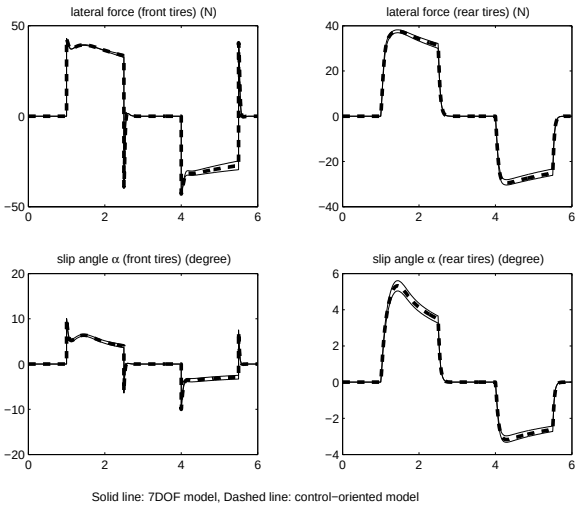

Fig. 6. Simulation results of the 7DOF model and the simplified model (b)

VII. Conclusions

This paper discusses Vehicle Stability Control for a vehicle with steer-by-wire and independently driven in-wheel motors. Its advantages over traditional VSC include more choice of inputs (including steering) and faster control with motors. A 7-DOF model was derived. However, the coupling of the inputs, and the nonlinearity and coupling of the tire forces makes it difficult to design VSC algorithms. A control-oriented modeling approach was taken and results in a model that is amenable for control and is capable of capturing the vehicle bahaviour. Control strategies were incorporated to decouple the longitudinal and lateral tire forces, and the steering and motor torques inputs. The proposed approach was validated by simulation results of both the 7-DOF model and the control oriented model.

References

[1] A. T. van Zanten. *Control aspects of the Bosch VDC.* AVEC'96, pp.573-608, Aachen, 1996

[2] A. T. van Zanten. *Bosch ESP Systems: 5 years of Experience.* SAE Technical Paper, 2000-01-1633

[3] Y. Hattori, K. Koibuchi. *Force and moment control with nonlinear optimum distribution for vehicle dynamics.* Toyota Central RD Labs

[4] M.Shino, Y.Wang. *Motion control of electric vehicles considering vehicle stability.* Tokyo University of Agriculture and Technology.

[5] Y.Hori, Y.Toyoda. *Traction control of electric vehicle: basic experimental results using the test EV "UOT Electric March".* IEEE Transactions on industry applications, Vol 34 1998.

[6] S.Sakai, H.Sado. *Motion control in an electric vehicle with four independently driven in-wheel motors.* IEEE Transactions of mechatronics, Vol.4, No.1, march 1999.

[7] H. Dugoff, P.S. Francher, and L. Segel. *An analysis of tire traction properties and their influence on vehicle dynamic performance.* SAE Document Number Document 700377, 1970

[8] S. Kueperkoch, J. Ahmed, A. Kojic and J-P. Hathout. *Novel vehicle stability control using steer-by-wire and independent four wheel torque distribution.* 2003 ASME International Mechnical Engineering Congress, Washington DC, 2003

[9] J.Y. Won, *Theory of Ground Vehicles.* Wiley-Interscience Publication, second addition, 1993

[10] A.T. van Zanten. *Evlolution of electronic control systems for improving the vehicle dynamic behavior.* AVEC, 2002